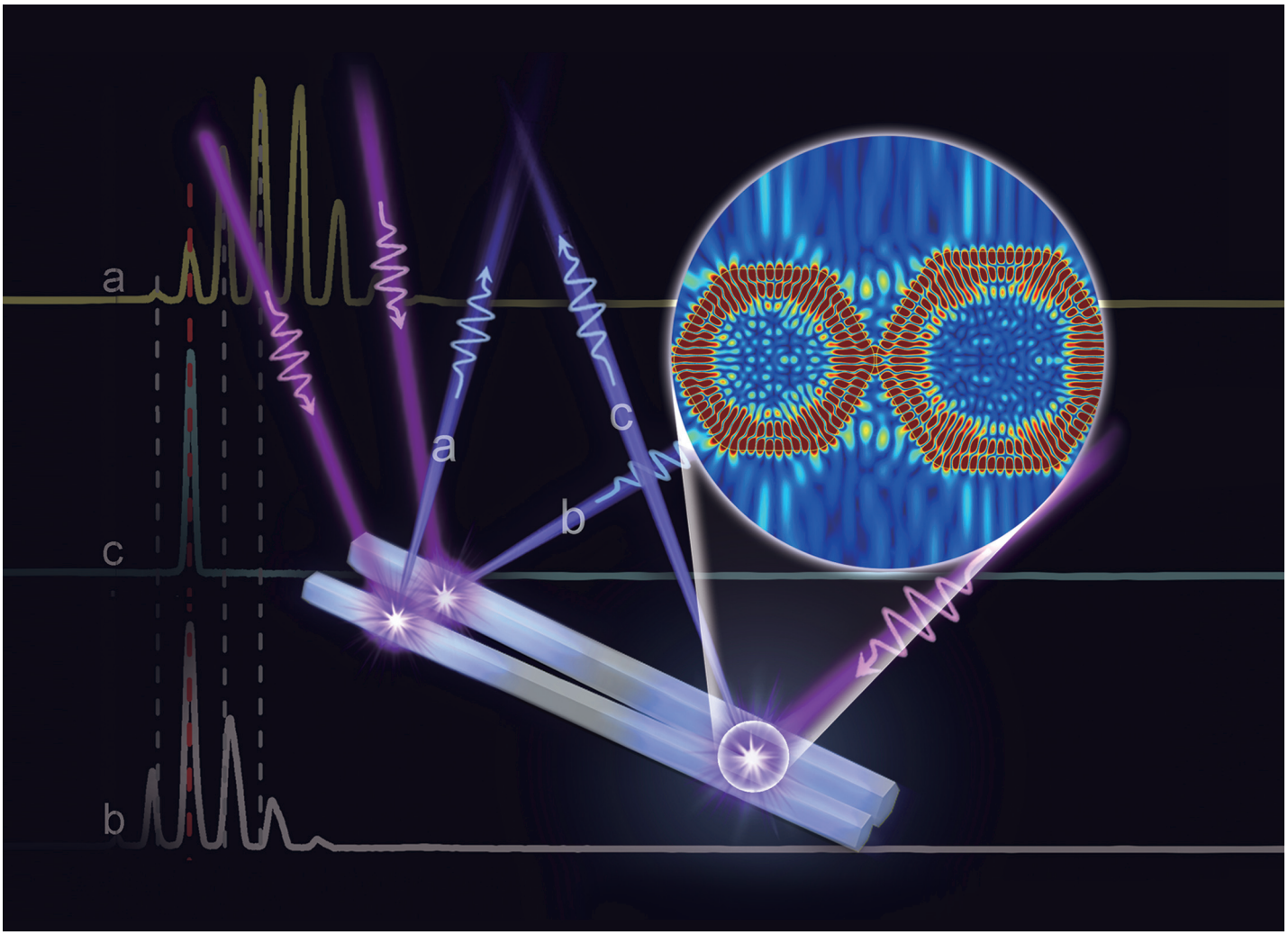

Showcasing research from the State Key Laboratory of Bioelectronics, School of Biological Science and Medical Engineering, Southeast University, Nanjing, China.

Lasing mode regulation and single-mode realization in ZnO whispering gallery microcavities by the Vernier effect

Two adjacent hexagonal ZnO microrods of a comb-like ZnO structure were designed as coupled whispering-gallery-mode cavities. Each individual ZnO microrod presented a multimode lasing structure. By regulating the nano-scale inter-space of coupled microrods, stable single-mode lasing with a higher Q factor and lower threshold was successfully obtained based on the Vernier effect. The theoretical and experimental investigations demonstrated the evolution process from multi-mode to single-mode lasing. This provides a general strategy for lasing mode modulation and single-mode operation.

As featured in:

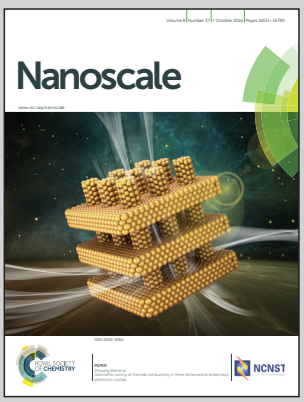

See C. X. Xu *et al.*, *Nanoscale*, 2016, **8**, 16631.

ROYAL SOCIETY OF CHEMISTRY

www.rsc.org/nanoscale

Registered charity number: 207890

Nanoscale

PAPER

View Article Online
View Journal | View Issue

Cite this: *Nanoscale*, 2016, **8**, 16631

Lasing mode regulation and single-mode realization in ZnO whispering gallery microcavities by the Vernier effect

Y. Y. Wang,[a,b] C. X. Xu,*[a] M. M. Jiang,[c] J. T. Li,[a] J. Dai,[a] J. F. Lu[a] and P. L. Li[a]

Received 20th June 2016,
Accepted 1st July 2016

DOI: 10.1039/c6nr04943e

www.rsc.org/nanoscale

The wide direct bandgap and strong exciton binding energy of ZnO have inspired examinations of ultraviolet lasing over the previous decades. However, regulation of the lasing mode, especially the realization of single mode lasing, is still a challenge. In this study, a ZnO comb-like structure with an array of microrods was selected to design coupled whispering-gallery-mode cavities, wherein the naturally varied air-gap between the adjacent microrods created a flexible condition for optical field coupling without any complicated micromanipulation. Spectral behaviour of lasing and coupling interaction between coupled ZnO microrods were systematically investigated. By regulating the nano-scale inter-space of dual coupled microrods, stable single-mode lasing with a higher *Q* factor and lower threshold was obtained successfully based on the Vernier effect. The formation conditions and the mechanism of single-mode lasing derived from the coupled ZnO microrods were discussed in detail. It also demonstrated an approach to construct high quality single-mode lasing by tuning the diameters of the coupled ZnO microrods.

1. Introduction

Whispering-gallery mode (WGM) nano/microscale lasers have attracted considerable attention for their high quality factors and low thresholds.[1–3] However, most of the reported lasing emissions presented multimodes due to a lack of mode selection capability, which would cause a group-velocity dispersion and lead to temporal pulse broadening and false signaling.[4] Therefore, it is significant to propose a critical technique for realizing the single-mode lasing (SML) output. This has many practical applications in optoelectronics, optical communication, high-density storage and acousto-optic deflector due to the advantages of low noise, good monochromaticity, long coherence length and high output power.[5,6] Therefore, it is urgent to achieve single mode lasing while retaining the merits of WGM-based nano/microscale lasers.

Several strategies have been proposed to realize single-mode lasing. A general way is the fabrication of distributed Bragg reflector mirrors[7] or distributed feedback gratings,[8,9] which involve fine optical design and complicated precise manufacture. Another approach is significantly reducing the cavity size of lasing to expand the free space range (FSR) of the multimodes until only one mode can exist in the resonant cavity. Based on this idea, Li *et al.* obtained a SML emission around 370 nm from a GaN nanowire with diameter of 135 nm.[10] However, the shortened dimension of the cavity inevitably increases the optical loss and deteriorates the laser quality (*Q*) factor, thus reducing the output energy, so very high pumping power is required to excite the SML. It is important to seek a better strategy to obtain the SML with a lower threshold and high quality. Fortunately, multimode suppression has been realized in the coupled-resonant cavities *via* the Vernier effect.[11] When two resonant cavities are coupled strongly to each other, only the coexistent lasing modes can occur due to the Vernier effect. The single-mode lasing action will generate when the greatly enlarged FSR exceeds the spectral width of the gain medium.[12] In fact, SML has been realized in various coupled WGM cavities *via* the Vernier effect such as silica/glass fibers,[13–15] optofluidic ring resonators,[16] microdisks,[17,18] and other nano/micro-scale semiconductor structures.[4,11,19,20] For instance, Gao *et al.* demonstrated a SML in cleaved-coupled single crystalline GaN nanowires by focused ion beam (FIB) milling to precisely design smooth endfaces and intercavity gap widths (as narrow as 30 nm) for strong coupling.[4] Through micromanipulation carried out by two fiber probes mounted on a precisely controlled 3-dimension moving stage under an optical microscope equipped with a super-long-distance objective lens, Xiao *et al.* converted a multi-

[a]*State Key Laboratory of Bioelectronics, School of Biological Science and Medical Engineering, Southeast University, Nanjing 210096, China. E-mail: xcxseu@seu.edu.cn*
[b]*School of Sciences, Zhejiang A&F University, Lin'an 311300, Zhejiang, China*
[c]*State Key Laboratory of Luminescence and Applications, Changchun Institute of Optics, Fine Mechanics and Physics, Chinese Academy of Sciences, Changchun 130033, China*

mode lasing into SML at around 738 nm by folding a 200 nm diameter CdSe nanowire to form the loop mirrors.[11] Xu *et al.* also obtained a single-mode UV lasing at around 370 nm from a pair of coupled GaN nanowires, which fabricated using a two-step top-down etch technique, including plasma etch and anisotropic wet etch.[19] Considering these researches, sophisticated micromanipulations, such as FIB milling,[4] chemical/reactive ion etching[19] and electron-beam lithography,[20] have generally been used to fabricate the appropriate coupled WGM cavities, which is crucial to achieve a SML by Vernier effect. To enlarge the scopes of applications in semiconductor materials, another alternative approach with practical fabrication and feasible operation are required to design coupled WGM cavities. This is beneficial for the realization of single mode lasing.

ZnO nano/microscale structures possessing natural optical resonant cavities[21,22] such as ZnO microrod with hexagonal cross section are an alternative WGM cavity to realizing high quality lasing. However, modulating output lasing modes, especially the realization of single mode lasing is still a challenge.[23] In this study, another alternative approach was proposed to construct suitable coupled ZnO WGM microcavities to obtain a UV SML with high Q factor and low threshold based on the Vernier effect. A comb-like ZnO structure with a microrod array was fabricated for the smart design of coupled WGM microcavities. This strategy has some advantages as follows. First, the comb-like ZnO structure can be synthesized efficiently by a simple vapour transport method. Second, each microrod has a perfect hexagonal cross-section that can act as an individual WGM cavity with good lasing performance. The last and most important is that the coupled microrods align parallel to each other with a gradually varied nano-scale air-gap from one end to other end. It provides a smart design to construct coupled WGM microcavities side-by-side, so the strong optical coupling can be achieved as well as the Vernier effect can be investigated systematically. Moreover, it eliminates the sophisticated manipulation to position two separate microcavities with nano-scale precision. In this case, high performance of the SML is expected through the optical coupling between the adjacent coupled microrods. Based on this strategy, the interaction between two-coupled microcavities is investigated systematically by the reliable and reproducible control of the SML. The lasing modes are regulated and the SML are achieved by adjusting the gap distance and diameter of coupled WGM microcavities. The condition of formation and mechanism of stable and single-mode emission are discussed in detail based on a systematic experiment and theoretical simulation.

2. Experimental details

2.1 Synthesis procedures

A comb-like ZnO structure was synthesized by a vapor phase transport method in a conventional horizontal tube furnace. In a typical experiment, the mixed powders of ZnO (purity 99.99%, purchased from Sinopharm Chemical Reagent Limited Corporation) and graphite (reducing agent, purchased from Huayuan Chemical Industry Limited Corporation, Shanghai) with a weight ratio of 2 : 1 were put into a small quartz boat as the source materials. A cleaned Si substrate was placed on the top of the quartz boat to collect the products. The quartz boat with the mixed powders and Si substrate was then placed into a quartz tube and placed in the high temperature zone around 1100 °C. The catalyst-free fabrication process indicates a vapor-solid mechanism in the growth procedure. The absence of catalyst particle also enables to fabricate the ZnO sample without any influence of impurities. Comb-like ZnO structure was obtained on the Si substrate after the reaction for 100 minutes in Ar (100 sccm) and O_2 (15 sccm) gases ambient.

2.2 Characterization

The morphology of the sample was characterized by field emission scanning electron microscopy (FESEM, Carl Zeiss Ultra Plus), which was equipped with energy dispersive X-ray spectroscopy (Oxford X-Max 50). The lasing from a coupled ZnO microrods was measured by a micro-PL system, wherein a femtosecond pulse laser (pulse duration 150 fs, repetition rate 1000 Hz, operates at 325 nm) was focused on the sample through an optical microscope (OLYMPUS BX53F) while the spectra and PL mapping were obtained through the optical multichannel analyzer (Acton SP2500i). The spectral resolution of the spectrometer is 0.025 nm, which is much smaller than the line width. The coupled ZnO microrods were excited simultaneously or individually depending on the excitation laser spot, which irradiating on the adjacent parts of the coupled microrods or an individual one. With the help of the CCD, it is not difficult to find a coupling position by moving the excitation spot along the wedged gap between two adjacent ZnO comb teeth. The excitation spot can move slightly along the wedged air gap with xy-axis translation stages. All the measurements were performed at room temperature.

3. Results and discussion

3.1 Numerical simulation results

The finite difference time domain (FDTD) numerical simulation was carried out to explore the optical field distribution in the coupled ZnO microrods, so that the coupling process can be understood clearly. As shown in the schematic in Fig. 1a, the incident light is perpendicular to the coupled hexagonal ZnO microrods, which have the diameters D_1 and D_2 of the circumscribing circles and are surrounded by air (n_{air} = 1). In the process of simulation, the effective index was introduced to simulate the optical field distribution in the hybrid cavity according to the optical waveguide theory. It is not only related to the material, but also to the structure and the surrounding media of the cavity. In other words, the effective index integrates the optical influences of the cavity dimension, interspacing of the two coupled cavities, and reflective indices

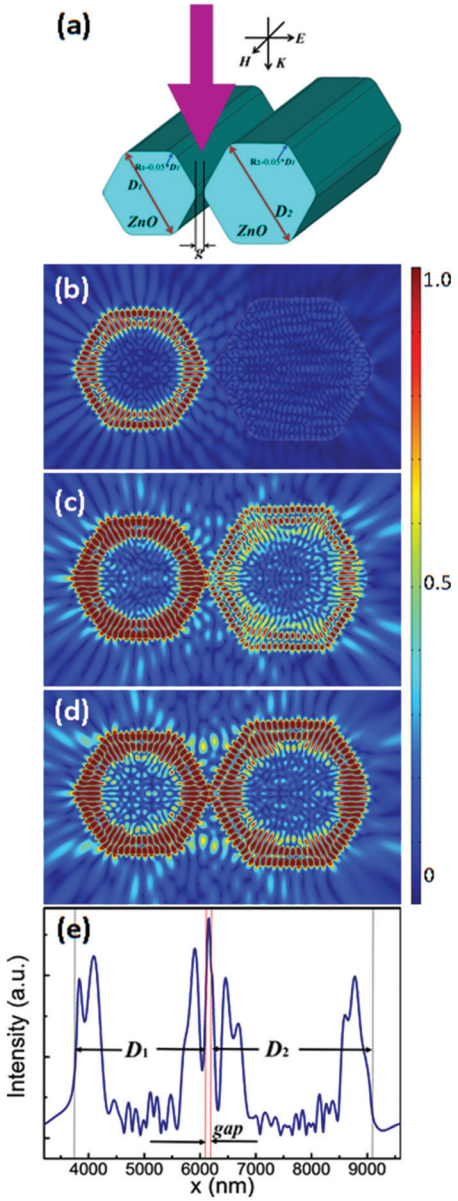

Fig. 1 (a) Schematic of two coupled ZnO microrods with D_1 = 2500 nm and D_2 = 3000 nm. (b) and (c) Normalized optical field distribution in the coupled microrods with air-gap g = 200 nm and 50 nm for the resonant wavelength at λ = 386.11 nm, corresponding to n_1 = 2.48, n_2 = 2.37. (d) Both microrods resonate at the same resonant wavelength λ = 387.64 nm corresponding to n_1 = n_2 = 2.45. (e) Energy distribution curves of the coupled microrods resonated at the same resonant wavelength.

of air and ZnO itself. The separation distance g denotes the air-gap between the two adjacent prism edges. As the leaking optical field includes both evanescent wave and the directly leaked part at the corners of the coupled hexagonal cavities, the separation distance may affect the optical field interaction.[24–27] The eigenvalue solver was used to find the resonant modes of the hybrid cavity. A similar simulation was also been carried out in other studies.[28,29] The transmission and reflection of photons are assumed to be absorbed eventually by the perfectly matched layers (PML). The mesh is defined as 2 nm. The simulations were performed on standard hexagonal cross section but with rounded edges to reduce the calculation amount of the FDTD simulation. This simplified configuration clearly demonstrates the optical field distribution of the individual or coupled cavities. In the experiments, the actual angular edges can induce more optical loss for an individual cavity but be favorable for inter-cavities optical field interaction because the light was easy to escape from the sharp angles. Qualitatively, the actual ZnO microrods with angular edges might have a similar resonant process with the proposed ones. Such fillet processing in simulations do not change the intrinsic optical properties of the WGM cavity, which has been commonly used in many reported studies.[30–33]

The optical field distributions in the coupled ZnO microrods are first simulated. Fig. 1b depicts the simulation result of a normalized optical field distribution inside a coupled cavity, which is composed of two ZnO microrods with different diameters (D_1 = 2500 nm and D_2 = 3000 nm) and a gap distance g = 200 nm. One of the typical resonant modes at λ = 386.11 nm for a smaller cavity was found, as shown by the resonant patterns in Fig. 1b. No resonant patterns appeared in the larger cavity, which indicates it cannot be on resonance at λ = 386.11 nm as the resonant condition of the bigger cavity is not satisfied. There is no occurrence of energy transfer from the smaller cavity to the larger adjacent one. It implies no optical field interaction happened as the two cavities are far enough. Optical field interaction occurs when the air-gap decreases to a small value (such as g = 50 nm). Some inhomogeneous patterns appeared in the larger microrod, whereas the smaller adjacent one is on resonance in its own mode, as shown in Fig. 1c. This indicates that the energy density of smaller cavity can be attenuated gradually due to energy transfer from the smaller cavity to the larger adjacent one through interaction. The bigger cavity likes a spectral filter to the resonance wavelengths of the adjacent smaller one. This explains why the lasing modes in the coupled cavities will be suppressed *via* the Vernier effect if they are not on resonance simultaneously. This is a key factor for SML realization to make both coupled ZnO microrods on resonance simultaneously at a coexistent wavelength of λ_i. By setting a similar effective refractive index of the coupled microrods to make their stimulated radiation spectral overlap, a coexistent resonant wavelength λ = 387.64 nm was found. This was verified by the perfect resonance patterns in both coupled microrods and the overlap optical field at the adjacent coupling region, as shown in Fig. 1d. The maximum intensities of energy distribution in the gap region, as shown red line region in Fig. 1(e), clearly displays the significant coupling between the two microcavities. As a result, in a coupled whispering gallery cavities, the lasing mode can be enhanced through coupling only if the lasing mode in the adjacent two cavities overlapped each other and are on resonance simultaneously. In addition, other non-overlapping modes will be depressed, and this phenomenon is known as the Vernier effect. This is one of the most important prerequisites to achieve a SML operation through

the Vernier effect if the coupled two microcavities hold only one coexistent mode.

3.2 Experimental results and discussion

Fig. 2a shows the morphology of an individual comb-like ZnO structure. This presents a microrod array with a length of 900 μm and a diameter of 3–12 μm aligned on one side of the ribbon-like stem with a width of 100 μm and a length of 800 μm. The enlarged SEM images reveal the hexagonal prisms of each microrod with inconsistent sizes and intervals, as shown in Fig. 2b. It retains the advantages of nanocomb, which are of interest for laser arrays,[34] biosensors,[35] and gratings.[36] The growth mechanism is similar to that of the nanocomb, as discussed in many previous reports.[37,38] Although the microrods array appears parallel to each other, it is noted that the interval of two adjacent microrods decreased tardily from the top of the microrod to the ribbon-like stem, which creates a natural and flexible condition for the systematic investigation on coupled WGM microcavities. Fig. 2c shows two typical microrods located side by side closely with a nano-scale air-gap between them. Such a special structure has its new application value. On the one hand, such a gradually varied nano-scale interval creates a flexible air-gap without any complicated micromanipulation to position the coupled microrods precisely. It is expedient to study the interaction between coupled ZnO microrods and find suitable coupled cavities to realize the controllable single-mode lasing. On the other hand, the perfect hexagonal facet morphology of the magnified coupled microrods indicates a good-performance WGM cavity with high lasing Q factor and low threshold.

Two closely located hexagonal ZnO microrods are selected to investigate the coupling behavior and explore the realization of single mode lasing. These two adjacent microrods with a slowly variable air gap are marked as A and B with a diameter of 6.6 μm and 7.4 μm, respectively, as shown in Fig. 3a. Each microrod can be pumped independently at the position with a sufficiently big air-gap. The UV lasing spectra in Fig. 3b for individual microrod under the pumping power of 200 kW cm^{-2} presents a clear Whispering-gallery multimode behaviour. As the excitation spot is located at position I, where the air-gap is 269 nm (see the right-up inset in Fig. 3a), both microrods A and B are pumped simultaneously. Fig. 3b also shows the representative lasing spectrum when two microrods are pumped simultaneously under the same excitation power as the individual cases. This lasing spectrum contains two groups of lasing modes obviously combining the contribution of both A and B. According to the plane wave model for resonant WGMs in hexagonal cavities, the exact positions of the lasing peaks can be calculated using the following equation:[2]

$$N = \frac{3\sqrt{3}nD}{2\lambda} - \frac{6}{\pi}\tan^{-1}\left(n\sqrt{3n^2-4}\right), \quad (1)$$

where n is the energy dependent refractive index and D is the diameter of the hexagonal cavities. The mode number N must be an integer, so that the lasing peak can be formed. The resonant modes of microrods A and B are related to the cavity size and the corresponding refractive index. It also depends on the excitation power if the lasing peak appears. The resonant modes of microrods A and B appear at different wavelengths due to the variation of the cavity size and the corresponding refractive index according to the mode number eqn (1). Fig. 3c shows that the mode number N originating from the microrod A is deduced as 103–109 and that of the microrod B is 109–114

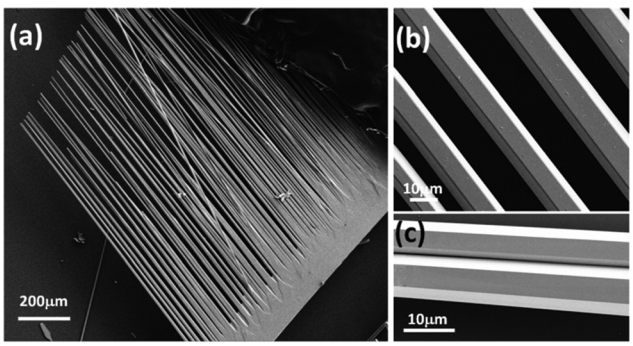

Fig. 2 (a) Typical SEM image of a comb-like ZnO structure. (b) The magnified SEM image of some microrods in the ZnO comb. (c) Typical two adjacent ZnO microrods in the ZnO comb.

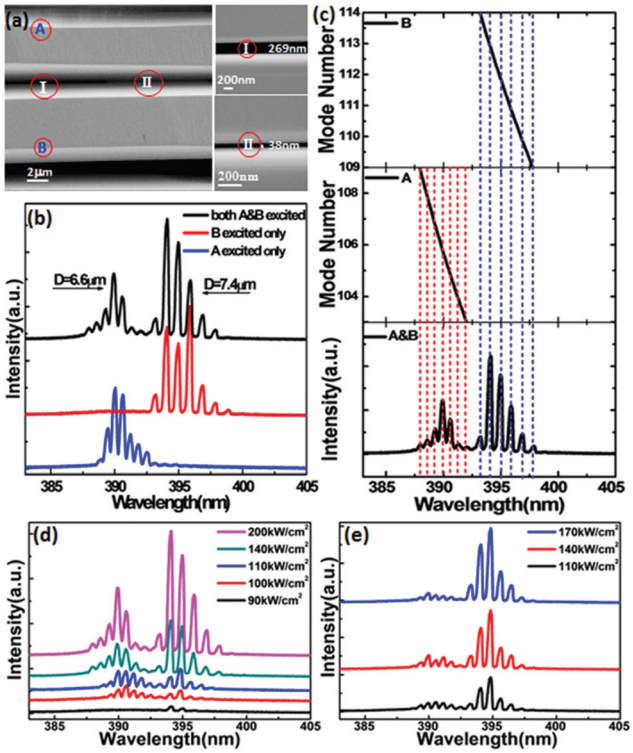

Fig. 3 (a) SEM image of two adjacent microrods A and B of the comb-like ZnO structure. The right insets are magnified images at positions I and II. (b) The representative lasing spectra from individual microrods A and B, and both of them at the position I under the same excitation power of 200 kW cm^{-2}. (c) Mode number figure of the lasing spectra excited at position I. The lasing spectra under different excitation power for both microrods A and B were excited simultaneously at positions I (d) and II (e).

under the same excitation power of 200 kW cm^{-2}, which proves the validity of the resonant wavelengths. It is well known that the Q factor plays a very important role in describing the laser cavity loss. For a lasing mode, the Q factor can be calculated with the formula,[39–41] $Q = \frac{\lambda}{\Delta\lambda}$, where λ and $\Delta\lambda$ denotes the resonance wavelength and its full width at half-maximum (FWHM), respectively. Based on the abovementioned equation and Lorentzian fitting, the lasing Q factor for a typical mode lasing of microrods A and B at 389.95 nm and 394.95 nm around the threshold is obtained as 1304 and 1479. This indicates that microrod B has a better optical field confinement ability than microrod A. Fig. 3d shows the lasing spectra under various pumping power for both microrods A and B, which are excited simultaneously at position I. At low pumping power, the lasing modes from the larger microrod B appear first because of its lower lasing threshold than that of the smaller one A. It can be explained by the gain threshold equation for WGM cavity expressed as $g_{th} = \alpha + [2/(3\sqrt{3}D)]\ln(1/R)^6$, where the first term is a total loss from the scattering, absorption, and transmission, whereas the second term is the reflective loss in the whispering gallery optical path with the reflectivity R on ZnO/air boundaries. Based on this equation, one can conclude that the threshold pumping power, P_{th}, is proportional to the gain threshold, g_{th}, which is therefore inversely proportional to the diagonal D. Fig. 3d also demonstrates that the lasing intensity of each microrod increases independently with increasing pumping power. No optical field interaction occurs between microrods A and B at the position I due to the large air-gap (269 nm). The experimental result agrees well with the simulation result displayed in Fig. 1b. The situation is dramatically different from the abovementioned case because these two microrods are simultaneously excited at the position II in Fig. 3a, wherein the air-gap is only 38 nm. The WGM lasing from microrods A and B also emerge simultaneously; however, the energy is redistributed in the two microrods, as clearly shown in Fig. 3e. This shows that the lasing intensity of microrod B increases more obviously with increasing pumping power than that of microrod A. This indicates optical field interaction may occur if the two microrods are very close to each other. It can be noted that the interaction distance in the experiment is slightly higher than that from the simulated geometry with a round edge because the angular edge makes the optical field easier to escape from the microcavities thus realizing interaction. Although optical field interaction happens in Fig. 3e, single mode lasing cannot still exist if each microrod is on resonance independently and the lasing spectra of two microrods have no overlapping, which is consistent with the simulation results.

The situation is quite different as some lasing modes coexist in two coupled microrods. Another two adjacent microrods C and D with diameters of D_1 = 6.4 μm and D_2 = 5.1 μm, as shown in the inset in Fig. 4a, are excited simultaneously at the position III wherein the air-gap is less than 60 nm. The double mode lasing peaks are located at 389.2 nm and

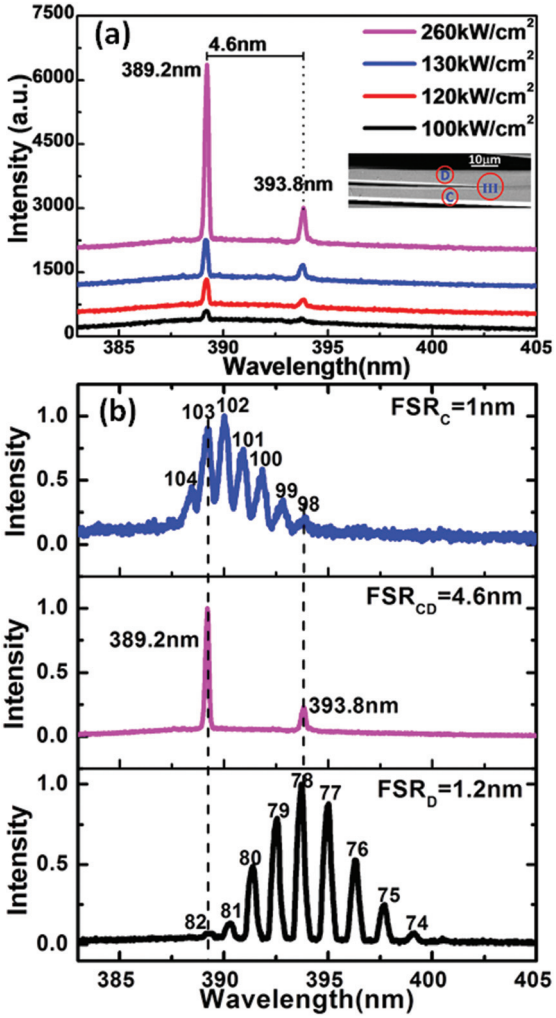

Fig. 4 (a) Double mode lasing from two coupled microrods C and D of the ZnO comb under different excitation power, the inset is its SEM image. (b) Normalized lasing spectra from the single microrod C, single microrod D, and coupled microrods at position III.

393.8 nm, which is always stable and no other emerging lasing peaks when increasing the lasing intensity with respect to the pumping power. The upper and bottom plots of Fig. 4b show that multiple modes arise from the individual microrod C and D when they are pumped separately at the far end with large air-gap from the ribbon stem of the comb-like ZnO structure. It is noted that some resonant modes coexist in both lasing spectra, which are just the two modes in Fig. 4a. In other words, only the coexistent modes resonate in the coupled microcavities, whereas the other non-concomitant modes disappeared. The mode spacing of WGM lasing from individual microrod C and D are 1 nm and 1.2 nm, respectively. When the two microrods pumped simultaneously at the position III, the mode spacing of the lasing from the coupled microcavity expends to 4.6 nm, which is much larger than that of individual C or D. The mode selection mechanism is attributed to the Vernier effect based on effective optical coupling between the two coupled microrods C and D at the position III, wherein the

air-gap is much less than the critical coupling distance (60 nm). Therefore, the evanescent wave from both microrods interacts efficiently. To verify the mechanism, the free spectral range (FSR) as a key parameter of the Vernier effect was analysed in detail. The FSR for the i^{th} individual hexagonal ZnO WGM microcavity is calculated by the following expression:[42]

$$\mathrm{FSR}_i = \frac{\lambda^2}{\frac{3\sqrt{3}}{2} D_i \left(n - \lambda \frac{\mathrm{d}n}{\mathrm{d}\lambda} \right)} \quad (2)$$

where n is refractive index of ZnO microrod arrays related to the wavelength, $(\mathrm{d}n/\mathrm{d}\lambda)$ is the dispersion relation and D_i is the i^{th} diagonal of the individual hexagonal microrod. The FSR for the coupled ZnO WGM cavity is estimated by the following Vernier equation:[43]

$$\mathrm{FSR}_{12} = \frac{\lambda^2}{\frac{3\sqrt{3}}{2} \left(n - \lambda \frac{\mathrm{d}n}{\mathrm{d}\lambda} \right) |D_1 - D_2|} \quad (3)$$

If the condition for observing the Vernier effect $M\mathrm{FSR}_1 = N\mathrm{FSR}_2$ is satisfied with integers M and N, the concomitant resonant modes in both microcavities will be amplified and the non-concomitant ones will be suppressed. The eqn (2) indicates that the FSR_i is not completely the same for different wavelengths. However, the coexistent resonant modes can still be found through the Vernier effect. Herein, a wavelength of 393.8 nm was chosen as an example. The theoretically calculated FSR_C, FSR_D and FSR_{CD} values are 0.948 nm, 1.192 nm and 4.65 nm, respectively. Thus, the Vernier effect can be fulfilled as $20 \times \mathrm{FSR}_{CD} = 98 \times \mathrm{FSR}_C = 78 \times \mathrm{FSR}_D$, which is satisfied based on the theoretical results. Our experimental results show FSR_C = 1 nm, FSR_D = 1.2 nm, and FSR_{CD} = 4.6 nm at the wavelength of 393.8 nm in Fig. 4b, which matches well with the theoretical results. The numerical calculation has been carried out and the mode number of each lasing peak, is shown in Fig. 4b, which clearly showed the corresponding mode structure by calculation thus successfully prove the satisfied Vernier effect. Fig. 4b also shows that only two overlapped peaks at 389.2 nm and 393.8 nm, which emerged in both individual microrod C and D and the coupled cavities, are enhanced by the Vernier effect, while other lasing modes at different wavelengths in individual cavities are suppressed, leading to the extension of FSR. Although FSR_i is not completely the same at different wavelengths, it will not hinder the Vernier effect from playing a role when the two lasing peaks are exactly overlapped.

According to eqn (3), FSR_{12} can be greatly enlarged if D_1 is in close proximity to D_2, so that only a single-mode can resonate inside the gain spectrum *via* the Vernier effect. Based on this, two coupled microrods E and F with similar diameters of 4.3 μm and 3.9 μm, respectively, were selected to motivate the corresponding lasing action, as shown in Fig. 5a. Single mode lasing can be obtained when both microrods were excited simultaneously at position IV with an air-gap as small as 45 nm, as shown in Fig. 5b. The SEM figure of other end of the microrod F is given to show that the diameter changes too little to affect the realization of single mode lasing based on the Vernier effect, as shown in Fig. 5c. Fig. 5d shows a stable single-mode operation over a large range of pumping power. The SML peak located at 390.4 nm with a side-mode suppression ratio (SMSR) of 19.7 dB. The SML action in Fig. 5d shows better performance than some reported literatures such as a SMSR of 15.6 dB in GaN nanowire-pairs,[19] 13.5 dB in coupled CdSe nanowire with loop mirrors structure,[11] and 14.6 dB in CdSe nanowire with X-structure.[44] The Lorentzian fitting of the spectrum demonstrates a FWHM of 0.21 nm. The single-mode lasing can exist stably with no occurrence of spectral mode-hoping. To confirm that the SML does not originate from the reduced single cavity size but from the Vernier effect, the critical dimension of a single cavity was calculated using the following formula:[45,46]

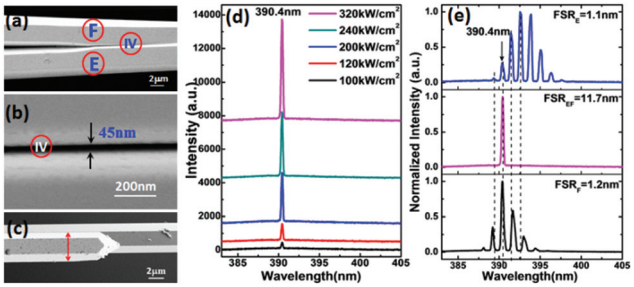

Fig. 5 (a) SEM image and (b) air-gap of the two microrods E and F. (c) SEM image of the other end of the microrod F. (d) The single mode WGM lasing from coupled microrods E and F of the ZnO comb under different excitation power. (e) The normalized lasing spectra from single microrod E and single microrod F and coupled microrods at position IV.

$$\frac{3\sqrt{3}}{2} \frac{D}{\lambda} \left({n_1}^2 - {n_2}^2 \right)^{\frac{1}{2}} \leq 2.405 \quad (4)$$

where D is a diameter of circle circumscribing the hexagonal microrod, λ is the wavelength in vacuum, and n_1 and n_2 are the refractive indices of the as-grown microrod array of the ZnO comb and the surrounding air, respectively. For the ZnO microrod, the critical diameter was estimated to be 172 nm for a resonant mode at 390.4 nm (n_1 = 2.46, and n_2 = 1.0) based on eqn (4), which is far smaller than the diameters of coupled microrods (4.3 μm and 3.9 μm) in our experiments. This calculation excludes the possibility of generating a SML in the individual microrod E or F because of their size, which is very large to satisfy the critical diameter of SML generation. Each individual ZnO microrod presents a multimode lasing structure, as shown in the upper and bottom plots of Fig. 5e. In our experiment, with the help of an optical microscope and *xy*-axis translation stages, the lasing spectrum of an individual cavity can be measured as close as possible to position IV just by moving the excitation spot slightly immediately upon the appearance of multimode. In this case, the diameter variation of E and F is negligible. In addition, the mode shift is very slow with respect to the cavity size. For example, a diameter

change of 200 nm just corresponds to the mode shift of 0.08 nm, which is such a small value compared to FSR and can be negligible. Actually, such a large change in diameter cannot occur in the measurement. Therefore, the mode shift caused by the variation in the cavity dimensions is negligible compared to FSR. These two spectra have only one coexistent resonance peak at 390.4 nm, whereas the other peaks are not fitted to each other. Efficient optical coupling was generated only when both microrods were excited simultaneously at position IV, wherein the air-gap between two microrods is only 45 nm. The estimated FSR_{EF} (11.7 nm) is not only larger than FSR of each microrod E or F (FSR_E = 1.1 nm and FSR_F = 1.2 nm), but also exceeds the spectral width of the gain medium for each microrod (7.1 nm and 6.3 nm), so that only one peak is allowed to exists in the coupled cavity. It can be inferred from simulation and experimental results that the single-mode operation based on Vernier effect involves two aspects: (1) the superposition of stimulated radiation spectra and closer diameters of ZnO microcavities make it possible to emerge some coexistent resonant wavelengths. In addition, other non-coexistent resonant modes will be suppressed. (2) The FSR of the lasing modes should be large enough to exceed the gain spectral width of ZnO to accommodate only one coexistent mode. These are the key factors for realizing the single mode lasing action based on the Vernier effect.

To optimize the performance of SML with a higher lasing Q factor and lower threshold, other smaller and larger coupled microrods are selected to investigate the influence on the optical characteristics of SML action. Three SMLs at 388.8 nm, 390.4 nm and 392.6 nm are obtained under the same excitation power of 240 kW cm^{-2}, as displayed in Fig. 6a. In addition to the aforementioned one at 390.4 nm in Fig. 5d, another two SMLs come from the coupled microrods with smaller diameters (D_1 = 3.1 μm, D_2 = 3 μm) and larger diameters (D_1 = 8.5 μm, D_2 = 8.3 μm), respectively. The side-mode suppression ratio (SMSR) of the three SMLs is 20.5 dB, 19.7 dB and 16.4 dB. The mode spacing is inversely related to the WGM cavity diameter. If the mode spacing is narrower, more lasing modes arise in the individual microrod with a larger diameter. More than one coexistence mode is more likely to emerge based on the Vernier effect. This leads to the lower SMSR of the single mode lasing from bigger coupled microrods. The FWHMs of the three SMLs around threshold are 0.28 nm, 0.26 nm and 0.13 nm, as well as the corresponding lasing Q factor around threshold are 1388, 1501 and 3020, respectively. The lasing Q factor of coupled microrods is similar to that of the individual microrod with a similar size. This indicates that the Vernier coupling still maintains the high lasing quantity of the individual perfect hexagonal microcavities. As a resonance enhancement of single mode lasing occurs in the two coupled microrods through coupling, more efficient utilization of energy in WGM microcavities can lead to lower optical loss. Based on Schawlow–Townes formula,[47] the FWHM becomes narrower due to lower optical loss; as a result, high lasing Q factor of SML will be obtained. Moreover, it shows that the larger coupled microrods display a higher

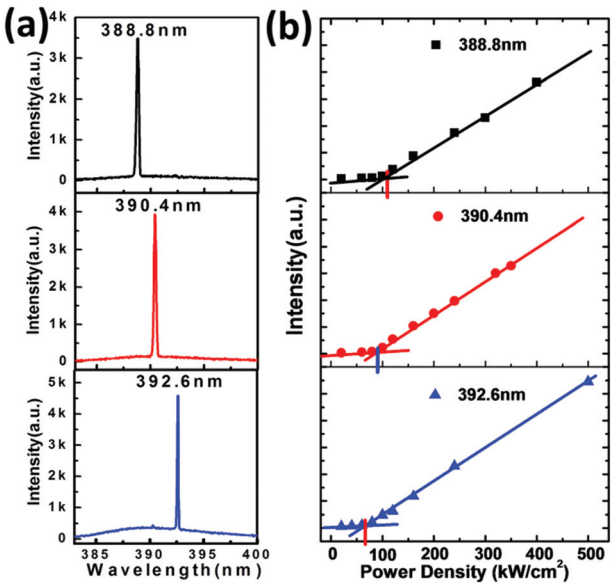

Fig. 6 (a) Three types of single mode lasing from different diameters of coupled microrods under the same excitation power of 240 kW cm^{-2}. The diameters of the coupled microrods are D_1 = 3.1 μm, D_2 = 3 μm (upper inset), D_1 = 4.3 μm and D_2 = 3.9 μm (middle inset) and D_1 = 8.5 μm, D_2 = 8.3 μm (bottom inset), (b) dependence of peak intensity on the excitation power of three types of single mode WGM lasing.

lasing Q factor than that of the smaller one. Previous study has shown that FWHM increases due to the increase in losses with decreasing cavity diameter.[30,48] Therefore, narrower FWHM and higher lasing Q factor of the single mode lasing is obtained in the larger coupled microrods due to the lower optical loss according to Schawlow–Townes formula. According to the output–input relation, the thresholds of the three SML were estimated to be 110 kW cm^{-2}, 90 kW cm^{-2} and 66 kW cm^{-2}, as shown in Fig. 6b. The largest coupled microrods show a lowest threshold. This demonstrates that the coupled microrods with larger dimension have better lasing performance such as stronger lasing intensity, higher lasing Q factor, narrower FWHM and lower threshold. As a result, the single mode lasing can be regulated by varying the coupled cavities size. Although the single mode lasing was achieved in coupled microrods based on pre-synthesized ZnO comb-like structure, it is feasible to achieve single mode lasing in any given coupled ZnO microrods by regulating the nano-scale air-gap artificially if the micromanipulation platform is available[11,49] as long as the conditions mentioned in this study are satisfied.

4. Conclusions

Comb-like ZnO structure with hexagonal prism microrod arrays was synthesized to design coupled whispering-gallery-mode cavities, wherein the naturally varied air-gap between two adjacent microrods created a flexible condition for optical field coupling without any complicated micromanipulation.

The critical coupling condition has been obtained theoretically and the simulation results verified the feasibility of single mode lasing through optical field coupling. Efficient coupling was designed experimentally to demonstrate the evolution process from multi-mode to double-mode and further to single-mode lasing. Based on the theoretical and experimental results, it is concluded that single-mode lasing can be accomplished successfully through the Vernier effect when the necessary and sufficient conditions are satisfied as follows: (1) the air-gap between two ZnO microrods should be less than the critical coupling distance (60 nm) so that the evanescent wave from both microrods can interact efficiently, (2) the lasing spectra of two microrods should have coexistent resonance modes, and (3) the FSR of coupled microcavities should be large enough to exceed the spectral width of the gain medium. The Vernier effect also demonstrates a facile approach to improve the lasing performance and tune the SML position by regulating the dimensions of the coupled microcavities. The proposed designing skills and the mode selection mechanism provided a general strategy for lasing mode regulation and single-mode realization.

Acknowledgements

This study was supported by "973" Program (2013CB932903), NSFC (61275054, 61475035, 11404289, 11574307, 11404328) and Opened Fund of the State Key Laboratory on Integrated Optoelectronics (2011KFJ004).

Notes and references

1 R. Chen, B. Ling, X. W. Sun and H. D. Sun, *Adv. Mater.*, 2011, **23**, 2199–2204.
2 C. Czekalla, C. Sturm, R. d. Schmidt-Grund, B. Cao, M. Lorenz and M. Grundmann, *Appl. Phys. Lett.*, 2008, **92**, 241102.
3 C. X. Xu, J. Dai, G. P. Zhu, G. Y. Zhu, Y. Lin, J. T. Li and Z. L. Shi, *Laser Photonics Rev.*, 2014, **8**, 469–494.
4 H. Gao, A. Fu, S. C. Andrews and P. Yang, *Proc. Natl. Acad. Sci. U. S. A.*, 2013, **110**, 865–869.
5 V. D. Ta, R. Chen, L. Ma, Y. J. Ying and H. D. Sun, *Laser Photonics Rev.*, 2013, **7**, 133–139.
6 Y. J. Lu, C. Y. Wang, J. Kim, H. Y. Chen, M. Y. Lu, Y. C. Chen, W. H. Chang, L. J. Chen, M. I. Stockman, C. K. Shih and S. Gwo, *Nano Lett.*, 2014, **14**, 4381–4388.
7 C. Sigler, J. D. Kirch, T. Earles, L. J. Mawst, Z. Yu and D. Botez, *Appl. Phys. Lett.*, 2014, **104**, 131108.
8 W. B. Huang, L. S. Chen and L. Xuan, *RSC Adv.*, 2014, **4**, 38606–38613.
9 B. Zhang, Z. R. Wang, S. Brodbeck, C. Schneider, M. Kamp, S. Hofling and H. Deng, *Light: Sci. Appl.*, 2014, **3**, e135.
10 Q. Li, J. B. Wright, W. W. Chow, T. S. Luk, I. Brener, L. F. Lester and G. T. Wang, *Opt. Express*, 2012, **20**, 17873–17879.
11 Y. Xiao, C. Meng, P. Wang, Y. Ye, H. K. Yu, S. S. Wang, F. X. Gu, L. Dai and L. M. Tong, *Nano Lett.*, 2011, **11**, 1122–1126.
12 E. M. Xu, X. L. Zhang, L. N. Zhou, Y. Zhang, Y. Yu, X. Li and D. X. Huang, *Opt. Lett.*, 2010, **35**, 1242–1244.
13 H. Zhu, S. F. Yu, Q. J. Wang, C. X. Shan and S. C. Su, *Opt. Lett.*, 2013, **38**, 1527–1529.
14 Y. G. Ma, X. Guo, X. Q. Wu, L. Dai and L. M. Tong, *Adv. Opt. Photonics*, 2013, **5**, 216–273.
15 V. D. Ta, R. Chen and H. Sun, *Adv. Opt. Mater.*, 2014, **2**, 220–225.
16 W. Lee, H. Li, J. D. Suter, K. Reddy, Y. Z. Sun and X. D. Fan, *Appl. Phys. Lett.*, 2011, **98**, 061103.
17 L. Mahler, A. Tredicucci, F. Beltram, C. Walther, J. Faist, B. Witzigmann, H. E. Beere and D. A. Ritchie, *Nat. Photonics*, 2009, **3**, 46–49.
18 A. Woolf, T. Puchtler, I. Aharonovich, T. T. Zhu, N. Niu, D. Q. Wang, R. Oliver and E. L. Hu, *Proc. Natl. Acad. Sci. U. S. A.*, 2014, **111**, 14042–14046.
19 H. W. Xu, J. B. Wright, T. S. Luk, J. J. Figiel, K. Cross, L. F. Lester, G. Balakrishnan, G. T. Wang, I. Brener and Q. M. Li, *Appl. Phys. Lett.*, 2012, **101**, 113106.
20 T. Grossmann, T. Wienhold, U. Bog, T. Beck, C. Friedmann, H. Kalt and T. Mappes, *Light: Sci. Appl.*, 2013, **2**, e82.
21 Y. Y. Lai, Y. P. Lan and T. C. Lu, *Light: Sci. Appl.*, 2013, **2**, e76.
22 P. K. Shrestha, Y. T. Chun and D. P. Chu, *Light: Sci. Appl.*, 2015, **4**, e259.
23 F. Schuster, B. Laumer, R. R. Zamani, C. Magen, J. R. Morante, J. Arbiol and M. Stutzmann, *ACS Nano*, 2014, **8**, 4376–4384.
24 X. Tu, Y.-K. Wu and L. Jay Guo, *Appl. Phys. Lett.*, 2012, **100**, 041103.
25 M. Ahmad and L. L. Hench, *Biosens. Bioelectron.*, 2005, **20**, 1312–1319.
26 L. Tong, R. R. Gattass, J. B. Ashcom, S. He, J. Lou, M. Shen, I. Maxwell and E. Mazur, *Nature*, 2003, **426**, 816–819.
27 L. Ren, X. Wu, M. Li, X. Zhang, L. Liu and L. Xu, *Opt. Lett.*, 2012, **37**, 3873–3875.
28 T. Holmgaard and S. I. Bozhevolnyi, *Phys. Rev. B: Condens. Matter*, 2007, **75**, 245405.
29 R. F. Oulton, V. J. Sorger, D. A. Genov, D. F. P. Pile and X. Zhang, *Nat. Photonics*, 2008, **2**, 496–500.
30 T. Nobis, E. Kaidashev, A. Rahm, M. Lorenz and M. Grundmann, *Phys. Rev. Lett.*, 2004, **93**, 103903.
31 H. Kudo, R. Suzuki and T. Tanabe, *Phys. Rev. A*, 2013, **88**, 023807.
32 B. Wang, X. Jin, H. Y. Wu, Z. Q. Zheng and Z. B. Ouyang, *Nanoscale*, 2014, **6**, 5338–5342.
33 D. Zhao, C. Zhang, X. X. Zhang, L. Cai, X. Zhang, P. S. Luan, Q. Zhang, M. Tu, Y. C. Wang, W. Y. Zhou, Z. Y. Li and S. S. Xie, *Nanoscale*, 2014, **6**, 483–491.
34 A. Manekkathodi, Y. J. Wu, L. W. Chu, S. Gwo, L. J. Chou and L. J. Chen, *Nanoscale*, 2013, **5**, 12185–12191.
35 J. X. Wang, X. W. Sun, A. Wei, Y. Lei, X. P. Cai, C. M. Li and Z. L. Dong, *Appl. Phys. Lett.*, 2006, **88**, 233106.
36 Z. W. Pan, S. M. Mahurin, S. Dai and D. H. Lowndes, *Nano Lett.*, 2005, **5**, 723–727.

37 C. X. Xu, X. W. Sun, Z. L. Dong and M. B. Yu, *J. Cryst. Growth*, 2004, **270**, 498–504.
38 X. B. Xu, M. Wu, M. Asoro, P. J. Ferreira and D. L. Fan, *Cryst. Growth Des.*, 2012, **12**, 4829–4833.
39 H. Zhu, Y. Fu, F. Meng, X. Wu, Z. Gong, Q. Ding, M. V. Gustafsson, M. T. Trinh, S. Jin and X. Y. Zhu, *Nat. Mater.*, 2015, **14**, 636–642.
40 M. Ding, D. Zhao, B. Yao, S. E. Z. Guo, L. Zhang and D. Shen, *Opt. Express*, 2012, **20**, 13657–13662.
41 A. K. Bhowmik, *Appl. Opt.*, 2000, **39**, 3071–3075.
42 H. Dong, Y. Liu, J. Lu, Z. Chen, J. Wang and L. Zhang, *J. Mater. Chem. C*, 2013, **1**, 202.
43 L. Shang, L. Y. Liu and L. Xu, *Opt. Lett.*, 2008, **33**, 1150–1152.
44 Y. Xiao, C. Meng, X. Q. Wu and L. M. Tong, *Appl. Phys. Lett.*, 2011, **99**, 023109.
45 X. F. Duan, Y. Huang, R. Agarwal and C. M. Lieber, *Nature*, 2003, **421**, 241–245.
46 D. F. Zhu, Q. G. He, Q. Chen, Y. Y. Fu, C. He, L. Q. Shi, X. Meng, C. M. Deng, H. M. Cao and J. G. Cheng, *ACS Nano*, 2011, **5**, 4293–4299.
47 S. Bartalini, S. Borri, P. Cancio, A. Castrillo, I. Galli, G. Giusfredi, D. Mazzotti, L. Gianfrani and P. De Natale, *Phys. Rev. Lett.*, 2010, **104**, 083904.
48 J. Wiersig, *Phys. Rev. A*, 2003, **67**, 023807.
49 X. Han, L. Kou, X. Lang, J. Xia, N. Wang, R. Qin, J. Lu, J. Xu, Z. Liao, X. Zhang, X. Shan, X. Song, J. Gao, W. Guo and D. Yu, *Adv. Mater.*, 2009, **21**, 4937–4941.